Journal of Quantitative Spectroscopy & Radiative Transfer ■ (■■■■) ■■■–■■■

Contents lists available at ScienceDirect

Journal of Quantitative Spectroscopy & Radiative Transfer

journal homepage: www.elsevier.com/locate/jqsrt

Accurate line intensities for water transitions in the infrared: Comparison of theory and experiment

Manfred Birk [a], Georg Wagner [a], Joep Loos [a], Lorenzo Lodi [b], Oleg L. Polyansky [b], Aleksandra A. Kyuberis [c], Nikolai F. Zobov [c], Jonathan Tennyson [b,*]

[a] Remote Sensing Technology Institute, German Aerospace Center (DLR), D-82234 Wessling, Germany
[b] Department of Physics and Astronomy, University College London, London WC1E 6BT, UK
[c] Institute of Applied Physics, Russian Academy of Sciences, Ulyanov Street 46, Nizhny Novgorod 603950, Russia

ARTICLE INFO

Article history:
Received 15 January 2017
Received in revised form
29 March 2017
Accepted 30 March 2017

Keywords:
Water
Absorption intensity
FTIR spectroscopy
Ab initio calculations

ABSTRACT

Ab initio calculations of water intensities are becoming mature and are claimed to have 1% accuracy in many cases. Experimental intensities with 1% accuracy can be achieved with some care. An intercomparison of *ab initio* against experimental water intensities is presented for a variety of infrared bands for $H_2{}^{16}O$ and some for $H_2{}^{18}O$ and $H_2{}^{17}O$. A new calculated $H_2{}^{16}O$ line list is presented for which uncertainties in the *ab initio* line intensities are evaluated. Much of the data show agreement within 2% between *ab initio* and experiment, however, for some bands, notably those involving excitation of some stretching modes, there are larger offsets of up to 8% attributed to *ab initio* calculation errors but still within the uncertainty of the *ab initio* calculation. In the ν_1 fundamental band differences of between +5% and −13% are found which show systematic dependence on wavenumber, ΔK_a, and ΔJ, again attributable to *ab initio* calculation errors. In the ν_2 band, intensity-dependent differences up to 2% originate from the analysis of the experimental data. At present experiments are important to validate *ab initio* calculations but *ab initio* predictions can be very useful in validating the experiment. As the two procedures display significantly different systematic errors, it is suggested that combining both gives the best results; this study will also facilitate further improvements of the theoretical methodology.

1. Introduction

Water is molecule number one in HITRAN [1], the major absorber of incoming sunlight in Earth's atmosphere and its biggest greenhouse gas. Its spectrum is therefore very well studied, see Refs. [2–7] for systematic compilations of experimental spectra of the various water isotopologues. However the demands of atmospheric science in general and satellite instruments such as MIPAS (Michelson Interferometer for Passive Atmospheric Sounding) on ENVISAT [8] mean that the laboratory data on water spectra must be of high quality. A particular issue is the reliability of the available transition intensities.

There are two approaches to obtaining accurate intensities for individual transitions. Traditionally this is done experimentally and there are a number of studies [9–11] which have produced intensity measurements which are accurate to 1% or better. For these measurements an extensive error analysis of systematic and random errors was carried out. In case of the 1 μm region, two independent measurements, those of Hodges et al. [10] and the DLR (German Aerospace Center) results included in HITRAN2012 [1], show intensities in agreement to better than 1% and within their combined uncertainties. In some cases, such high-accuracy measurements comprise only a few selected lines and therefore serve as a benchmark rather than a dataset suitable for inclusion in standard databases. The intention of laboratory spectroscopy work at DLR is to provide spectroscopic data with small well-defined uncertainties. This is certainly true for H_2O spectroscopy, as well. Laboratory infrastructure such as absorption cells have been continuously improved together with analysis software. Special focus was placed on validation of data product accuracy, *i.e.* proving the error budget by redundancy, χ test and so forth [12]. More details are given in Section 2 which details our experimental studies on water line intensities.

The second approach is to make use of the increasing accuracy of *ab initio* calculations. A number of studies have focussed on trying to determine the dipole moment surface (DMS) of the water molecule to high accuracy [13–16]. However, computed vibration-rotation transition intensities are also sensitive to the nuclear-motion wavefunctions of the initial and final state, and hence to the potential energy surface (PES). Lodi and Tennyson [17]

* Corresponding author.
E-mail address: j.tennyson@ucl.ac.uk (J. Tennyson).

http://dx.doi.org/10.1016/j.jqsrt.2017.03.040

Table 1
Overview of H_2O intensity measurements performed at DLR. Experiment are numbered and referred to in the text as Expt. *N*.

N	Year	Spectral region (cm^{-1})	Refs.	Purpose	Profile[a]	Fit[b]	Funded by
1	2003–05	1250–1750	[20,12]	MIPAS/ENVISAT	Voigt	Single	HGF national
2	2006–07	10,000–11,000	[1]	WALES	SD-Voigt	Single	DLR project national
3	2016	1850–2280, 2390–4000	[21–23]	NDACC, TCCON	QSDHC+LM	Multi	DFG national
4	2016	4190–4340	[24,25]	TROPOMI/Sentinel 5-P	QSDHC+LM	Multi	ESA

[a] SD-Voigt: Speed-Dependent Voigt; QSDHC+LM: quadratic-Speed-Dependent Hard-Collision profile plus Rosenkranz line-mixing.
[b] Single spectrum or multi-spectral fits.

developed a procedure to test for sensitivity of the results to both the PES and DMS. The results of such a procedure are analyzed below. Lodi and Tennyson's computed intensities formed the major input into HITRAN2012 [18] for the water isotopologues $H_2{}^{18}O$ and $H_2{}^{17}O$. A subsequent experimental validation of HITRAN2012 yielded generally good agreement with these results in the 6450–9400 cm^{-1} region [18].

Clearly there is a case for considering a similar treatment for the main water isotopologue, $H_2{}^{16}O$, whose spectrum is crucial for atmospheric and many other applications. However, given the volume of experimental work on $H_2{}^{16}O$ spectra and that measurements for the main isotopologue can generally be made more accurately due to its high natural abundance, it is necessary to properly benchmark the *ab initio* intensities for this system. This is the purpose of the present paper which, indeed, demonstrates that while the *ab initio* predictions are excellent in many cases there are a number of bands which display systematic differences from observation which are too large for these data to be used in the present form.

The paper is organized as follows. The following section describes the experimental studies performed at DLR against which the *ab initio* intensities are benchmarked. Section 3 outlines our theoretical procedure and presents a new, high-accuracy line list for $H_2{}^{16}O$ which includes uncertainties for the line intensities. Section 4 presents a detailed band-by-band comparison between the two sets of line intensities. Finally we present our conclusions. All experimental intensities and the intercomparisons shown in the paper include HITRAN's isotopologue abundance – unless specified otherwise. The *ab initio* intensities in the Supplementary material are given for 100% abundance.

2. Experimental water line intensities

The hardware in the DLR spectroscopy laboratory was developed over 25 years with a focus on prevention of systematic errors. Absorption cells cover path lengths, *L*, from 20 cm to 200 m and a temperature range from 195 to 350 K. Special care has been taken to achieve high temperature homogeneity. The Fourier Transform (FT) spectrometer was originally a Bruker IFS 120HR, which was upgraded to a Bruker IFS 125HR in 2009. Due to the high spectral resolution, the influence of the instrumental line shape can be minimized, which helps avoiding systematic errors. As sample gas evaporated water vapor from a liquid tap water reservoir was used. The water was purified prior to usage by freezing it several times using liquid nitrogen and pumping off the gas phase. During the sample gas evaporation process only water contributed significantly to the vapor phase. Especially in case of water and water/air mixtures steady flows have been used to counter the effects of wall stickiness. Water/air mixtures are generated in an 800 l stainless steel vessel for high mixing ratio accuracy. High accuracy pressure and temperature sensors are employed. Spectral processing corrects for several systematic error sources such as detector non-linearity, sample and cell window thermal radiation, and standing waves in the optics. The measurement plan includes sufficient redundancy, *e.g.* the same transition is measured with different optical depths. Redundancy helps to find unidentified systematic errors since the impact of error sources mostly changes with optical depth, sample and total pressure, mixing ratio, temperature and absorption path. Measurement conditions are selected to match the requirements from atmospheric spectra. Several methods were developed for validation of data product accuracy. For example, gas temperatures are fitted from relative line intensities and compared to sensor temperatures. Furthermore, residuals are investigated with respect to single measurements, called file cuts [19]. More details on methods for validation of data product accuracy can be found in [19].

A list of all DLR H_2O experiments contributing to this work, sorted by date, is given in Table 1. These experiments are detailed in turn below.

Expt. 1: The FT instrument was a Bruker IFS 120HR. The old multireflection cell setup with unoptimized temperature homogeneity and 100 m maximum absorption path was used. Nine pure H_2O ($L = 0.25 - 85$ m, $p_{H_2O} = 0.2 - 5$ mbar, ambient temperature, 0.6/MOPD = 0.0032 cm^{-1}) and 14 air-broadened measurements ($L = 21 - 85$ m, $p_{H_2O} = 0.2 - 5$ mbar, $p_{air} = 50 - 400$ mbar, ambient temperature, 0.6/MOPD = 0.0032 cm^{-1}, for relative line intensities only) were used for intensity analysis. Line parameters were retrieved with FitMAS [26] in single spectrum Voigt fits with *sinc* ⊗ *box* idealized instrumental lineshape and afterwards merged together. The number of lines with statistical uncertainty ≤1% was 579 for the main isotopologue in the line intensity range 2×10^{-23}–3×10^{-19} cm molecule^{-1}, and 276 for $H_2{}^{18}O$ (statistical uncertainty ≤5%) in the line intensity range 5×10^{-25}–7×10^{-22} cm molecule^{-1}, including lines of the ν_2 fundamental and its first hot band. Spectral lines for this region are given in Supplementary data as two files: one each for $H_2{}^{16}O$ and $H_2{}^{18}O$. This region has been the subject of a number of studies by Toth [27–29] which formed the basis of input to previous versions of HITRAN and Coudert et al. [30] which provided the input to the recent GEISA update [31].

Expt. 2: The FT instrument was a Bruker IFS 120HR. The old multireflection cell setup was used. Two pure H_2O (L=85 m, $p_{H_2O} = 1 - 5$ mbar, ambient temperature, 0.6/MOPD = 0.03 –0.013 cm^{-1}) and nine air-broadened measurements (L=85 m, $p_{H_2O} = 0.8 - 16.4$ mbar, $p_{air} = 200 - 1000$ mbar, ambient temperature, 0.6/MOPD = 0.06 – 0.03 cm^{-1}, for relative line intensities only) were used for intensity analysis. Line parameters were retrieved with an IDL single spectrum speed-dependent Voigt [32] fit with *sinc* ⊗ *box* idealized instrumental lineshape and afterwards merged together. The number of lines analyzed with statistical uncertainty ≤ 1% was 326 for the main isotopologue in the line intensity range 1×10^{-24}– 6.5×10^{-22} cm molecule^{-1}, including lines of the bands from (0 0 0) to (1 2 1), (2 2 0), (3 0 0), (2 0 1), (0 0 3) and (1 0 2). Spectral lines for this region are given in Supplementary data. The 1% accuracy achieved represents a significant improvement on previous state-of-the-art studies of this region [33–35].

Expt. 3: The FT instrument was a Bruker IFS 125HR. A short absorption path cell (L=24.9 cm) and the refurbished

Please cite this article as: Birk M, et al. Accurate line intensities for water transitions in the infrared: Comparison of theory and experiment. J Quant Spectrosc Radiat Transfer (2017), http://dx.doi.org/10.1016/j.jqsrt.2017.03.040

multireflection cell setup was used. 15 pure H_2O measurements ($L = 0.249 - 176$ m, $p_{H_2O} = 0.1 - 20$ mbar, ambient temperature, 0.6/MOPD = 0.0024 – 0.0033 cm^{-1}) were used for intensity analysis. Line parameters were retrieved with an IDL multispectrum fit using a quadratic speed-dependent hard collision (QSDHC) lineshape model [36–40] extended for Rosenkranz line mixing. Besides positions and intensities, self-broadened lineshape parameters (speed-dependence, shift and in a few cases line mixing) were fitted. The instrumental lineshape was characterized using Doppler-broadened N_2O measurements analyzed with the LINEFIT software [41]. 2224 lines with statistical uncertainty $\leq 1\%$ were analyzed for the main isotopologue in the line intensity range 3.5×10^{-27}–2.5×10^{-19} cm $molecule^{-1}$, 403 for $H_2{}^{18}O$ in the range 1.7×10^{-26}– 4.8×10^{-22} cm $molecule^{-1}$ and 172 for $H_2{}^{17}O$ in the range 1.4×10^{-26}– 9.2×10^{-23} cm $molecule^{-1}$, including lines of the bands ν_1, ν_2, $2\nu_2$, ν_3, (1 1 0)–(0 1 0), (0 3 0)–(0 1 0), (0 1 1)–(0 1 0), (0 0 1)–(0 1 0) and (1 0 0)–(0 1 0). For every parameter of each line errors from various sources (pressure measurement, temperature measurement, cell length, …) were propagated into the final line parameter uncertainties. A root-mean-square (rms) value from statistical and all propagated systematic errors was formed to obtain a single combined accuracy for each fitted parameter. Spectral lines for this region are given in another paper in this issue [22]. Earlier studies of water absorption in this region have been performed by Toth [29,42] and others [43,30]. Comparisons with other experimental studies are given in Ref. [22].

Expt. 4: The FT instrument was a Bruker IFS 125HR. The refurbished multireflection cell setup was used. 6 pure H_2O measurements ($L = 14.6 - 204.5$ m, $p_{H_2O} = 0.75 - 20$ mbar, $p_{tot} = 30 - 1000$ mbar, ambient temperature, 0.6/MOPD = 0.004 cm^{-1}) and 16 air broadened measurements (L=59.2 and 168.2 m, $p_{H_2O} = 0.2 - 23$ mbar, ambient temperature, 0.6/MOPD = 0.004 – 0.012 cm^{-1}) were used for simultaneous analysis of positions, intensities and air- and self-broadened lineshape parameters using an IDL multispectrum fit and a QSDHC lineshape model extended for Rosenkranz line mixing. Besides positions and intensities air- and self-broadened lineshape parameters (speed-dependence, Dicke-narrowing, shift and in some cases line mixing) were fitted. The instrumental lineshape was characterized using Doppler-broadened CO measurements analyzed with the LINEFIT software [41]. 144 lines were analyzed for the main isotopologue in the line intensity range 7.8×10^{-27}–3.5×10^{-25} cm $molecule^{-1}$, 9 for $H_2{}^{18}O$ in the range 3.2×10^{-26}–3.3×10^{-22} cm $molecule^{-1}$ and 1 for $H_2{}^{17}O$ with the intensity 4.7×10^{-26} cm $molecule^{-1}$, including lines of the bands ν_1, ν_2, $2\nu_2$ and (0 1 1)–(0 1 0). Spectral lines for this region are given in Supplementary data. Recent studies in this region can be found in Refs. [30,44,45].

3. Theoretical line intensities

From a theoretical standpoint transition intensities, in cm $molecule^{-1}$, can be calculated using the expression

$$I_{if} = 4.162034 \times 10^{19} \omega_{if} g_i Q^{-1}(T) \left[\exp\left(\frac{-c_2 E_i}{T}\right) - \exp\left(\frac{-c_2 E_f}{T}\right) \right] \left| \sum_{\alpha} \langle i|\mu_{\alpha}|f\rangle \right|^2 \quad (1)$$

where T is the temperature, c_2 is the second radiation constant, $\omega_{if} = E_f - E_i$ is the transition frequency between the i'th and f'th state (all in cm^{-1}), and g_i is the total degeneracy factor. E_i and E_f are the initial and final energy levels, which for the states considered here have been accurately determined using empirical data [2–6]. The partition function, $Q(T)$, for water has been determined to high accuracy [46,47] and therefore does not contribute significantly to the uncertainty. The final sum represents the line strength which must be calculated. To do this requires initial, $|i\rangle$ and final, $|f\rangle$ rotation-vibration wavefunctions as well the DMS, μ_α. For water, the DMS is two-dimensional vector since there is no component of the dipole outside the plane of the molecule.

The procedure used to construct a list of reliably-predicted line intensities for $H_2{}^{16}O$ relies heavily on the principles of uncertainty quantification in atomic and molecular calculations [48] and, in particular, was based on the study of $H_2{}^{18}O$ and $H_2{}^{17}O$ by Lodi and Tennyson [17]. Lodi and Tennyson realized that, for high accuracy calculations, the dominant uncertainty in predicting the intensity of the majority of spectral lines is the quality of the underlying DMS. However, for lines where either the initial or final state is involved in an accidental resonance, inaccuracies in the computed wavefunctions make it difficult and, in some cases, impossible to compute a reliable intensity. The Lodi-Tennyson method therefore uses multiple calculations to assess the stability of a given line to resonances. If the line is deemed stable, then the uncertainty in the intensity is assumed to arise from the underlying DMS; otherwise, significantly larger uncertainty estimates are adopted. Detailed discussions of the procedure can be found in the original paper by Lodi and Tennyson [17] and more recent analysis on CO_2 line intensities by Zak et al. [49–51]. Finally it is worth noting that DMSs derived from *ab initio* calculations cannot be expected to be uniformly accurate for all bands. It is characteristic of these surfaces that, in the absence of accidental resonances, a given DMS reproduces all transitions within a given vibrational band with a rather uniform accuracy but that this accuracy may differ between bands. This manifests itself as systematic shifts when computed intensities are compared with measured ones. Conversely the observation of unexpected, systematic structures within a given band has been used to identify problems with the fits of observed high accuracy CO_2 spectra [49–51]. Finally it should be noted that since non-Born-Oppenheimer correction to the DMS is known to be small [52], the DMS used here was computed assuming the Born-Oppenheimer approximation [16]. This means that the DMS should be equally valid for all isotopologues of water.

In this work calculations were performed with the best available spectroscopically-determined PES due to Bubukina et al. [53] (henceforth Bubukina2011) and the high quality CVRQD *ab initio* PES due to Barletta et al. [54]. Two different DMS based on separate fits to the same high accuracy *ab initio* calculations of Lodi et al. [16]: LTP2011 is a tightly converged fit while LTP2011S is a fewer-parameter fit designed to safe-guard against artificial structures being produced in the surface due to over-fitting [14,55]. Our base model, which is used to provide the predicted line intensities is (Bubukina2011,LTP2011). Line lists were also computed with the other 3 possible combinations of the PESs and DMSs. These line lists were used to test the stability of the base model with respect to changes in the vibration-rotation wavefunction (which depend on the PES) and dipole surface (*i.e.* DMS). For transitions which are stable under these circumstances, it is assumed on the basis of previous analysis and tests [16,56] that line intensities are accurate to 1%. Lines which proved not be stable under these test are assigned significantly higher uncertainties on a case-by-case basis.

The nuclear motion calculations were performed with the DVR3D program suite [57] in Radau coordinates and a bisector embedding. The calculations considered rotational states with J up to 25. Transitions up to 20,000 cm^{-1} were considered. Water absorption spectra with higher frequency than this are well-known [58–60] but there are underlying issues with the representation of the DMS and associated transition intensities for these high quanta transitions [61,62]; we leave the study of this region for future work.

Our final $H_2{}^{16}O$ line list contains all transitions with an intensity higher than 10^{-29} cm $molecule^{-1}$ and $J \leq 24$ at 296 K with no scaling to natural abundance. It contains 141,839 lines and a file with these lines is given in Supplementary data.

Please cite this article as: Birk M, et al. Accurate line intensities for water transitions in the infrared: Comparison of theory and experiment. J Quant Spectrosc Radiat Transfer (2017), http://dx.doi.org/10.1016/j.jqsrt.2017.03.040

4. Intercomparison of experimental and theoretical data

Intercomparisons are discussed in the order given in Table 1.

4.1. 1250–1750 cm^{-1}

As already mentioned, the experimental data in this region were analyzed with a Voigt profile. From subsequent experience with profiles including collisional narrowing and speed dependence, we cannot exclude systematic errors. This is especially true in our case since relative intensities of air-broadened measurements were also fed into the analysis together with pure water measurements. Furthermore, experimental line intensities above 10^{-23} cm molecule^{-1} were analyzed by Coudert applying an effective Hamiltonian (EH) approach [20], including experimental line intensities for other bands from other sources. The results from the EH approach were added into HITRAN2008 [63] and were retained in HITRAN2012 [1]. The experimental values presented here are slightly improved compared to the data used for the EH approach, leading to small differences (< 0.5%) for strong lines. For intercomparison the *ab initio* values were scaled with 0.9976 since they are given for pure isotopologues while the experimental values are given for the natural isotopologue mixture.

Fig. 1 shows the percentage differences between *ab initio* and experimental line intensities together with total uncertainties, including lines with statistical uncertainties limited to a maximum of 1%. The total uncertainties as listed by Coudert et al. [20] and shown in Fig. 1 were generated by multiplying the statistical uncertainty with the dimensionless standard deviation χ, both resulting from the averaging of line intensities from single spectrum analyses. Furthermore, 1% systematic uncertainty accounting for pressure and temperature uncertainties was added. For 90% of the transitions with statistical uncertainty less than 1%, χ was below 2 and for 70% below 1.6. χ being somewhat larger than 1 indicates the presence of systematic errors.

Table 2 gives the average differences, called offsets, for different line intensity ranges, again using only intensities with statistical uncertainties less than 1%. The difference is about 2% for strong lines and decreases to 0.7% for lines with intensity of about 10^{-22} cm molecule^{-1}. For weaker lines the difference increases again. In Fig. 2 the differences for the ν_2 fundamental are sorted by line intensity and the *ab initio* uncertainty is given. Fig. 3 shows the same information for the first hot band of ν_2. The *ab initio* uncertainties for the hot band are larger than for the fundamental but still well below 1% and thus below the experimental uncertainties. The differences between *ab initio* and experimental intensities are mostly within the experimental uncertainties.

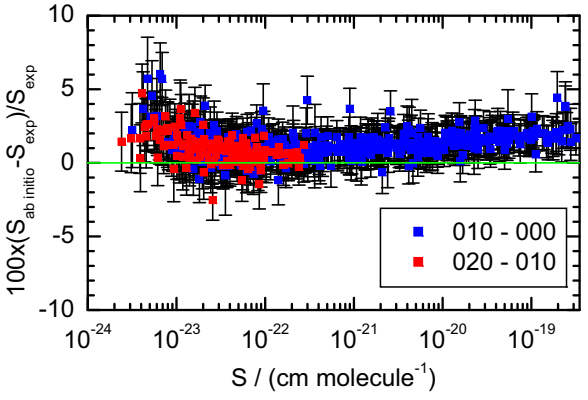

Fig. 1. Percentage *ab initio*–experimental *vs.* intensity, bands (0 1 0)–(0 0 0) and (0 2 0)–(0 1 0) of $H_2{}^{16}O$. Statistical error limit of experimental data 1%. The error bars indicate the total experimental uncertainties.

Table 2
Percentage *ab initio*–experimental for intensity ranges, bands (0 1 0)–(0 0 0) and (0 2 0)–(0 1 0) of $H_2{}^{16}O$. Statistical error limit of experimental data 1%. Offset error denotes the statistical uncertainty of the offset.

log(S_{min})	log(S_{max})	Offset/%	Offset error/%	No. lines
−24.0	−23.5	1.55	0.11	2
−23.5	−23.0	2.40	0.22	41
−23.0	−22.5	1.14	0.11	87
−22.5	−22.0	0.71	0.07	109
−22.0	−21.5	0.76	0.08	69
−21.5	−21.0	0.94	0.09	48
−21.0	−20.5	1.15	0.08	52
−20.5	−20.0	1.21	0.08	51
−20.0	−19.5	1.61	0.07	49
−19.5	−19.0	1.76	0.05	44
−19.0	−18.5	2.13	0.16	27

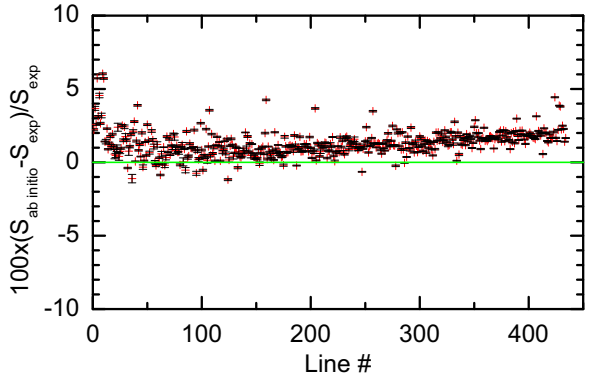

Fig. 2. Percentage *ab initio*–experimental *vs.* line number, sorted by intensity, band (0 1 0)–(0 0 0) of $H_2{}^{16}O$. Statistical error limit of experimental data 1%. The error bars indicate the *ab initio* uncertainties.

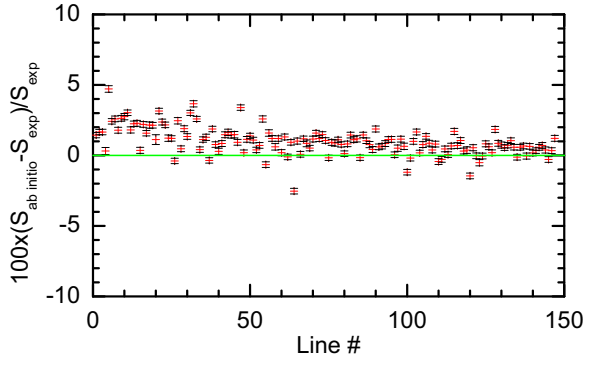

Fig. 3. Percentage *ab initio*–experimental *vs.* line number, sorted by intensity, band (0 2 0)–(0 1 0) of $H_2{}^{16}O$. Statistical error limit of experimental data 1%. The error bars indicate the *ab initio* uncertainties.

Fig. 4 compares the *ab initio* results with those of the EH approach between 1250 and 1750 cm^{-1}, as contained in HITRAN 2008 and 2012. Table 3 gives the average differences for different line intensity ranges, analogous to Table 2. The line intensities from HITRAN were taken from EH calculations based on experimental intensities greater than 10^{-23} cm molecule^{-1}.

In the intensity range where experimental data were available the differences are, in contrast to the experimental data, almost constant ranging from 1.4% to 1.6%. The differences are in reasonable agreement to the direct intercomparison with the experimental data (Table 2), *i.e.* the EH approach can represent the experimental data within 0.5% on a relative basis. For the weaker lines, however, larger differences up to 20% occur which increase with decreasing line intensity. For HITRAN2012 data above 1750 cm^{-1} the EH data used in HITRAN is not

Please cite this article as: Birk M, et al. Accurate line intensities for water transitions in the infrared: Comparison of theory and experiment. J Quant Spectrosc Radiat Transfer (2017), http://dx.doi.org/10.1016/j.jqsrt.2017.03.040

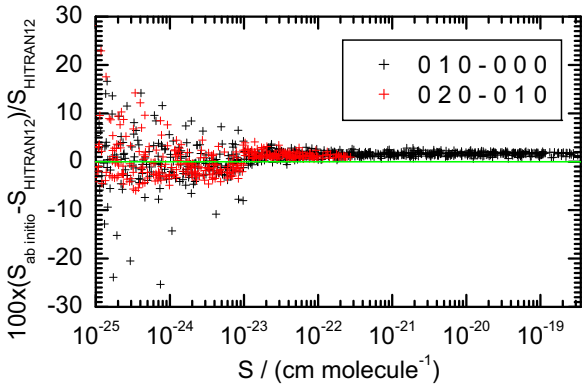

Fig. 4. Percentage *ab initio*–HITRAN2012 *vs.* intensity, bands (0 1 0)–(0 0 0) and (0 2 0)–(0 1 0) of $H_2{}^{16}O$. Wavenumber range corresponding to Table 2 1250–1750 cm^{-1}. The discontinuity at 10^{-23} cm molecule^{-1} is caused by the intensity limit of experimental data entered into the effective Hamiltonian fit.

Table 3
Percentage *ab initio*–HITRAN2012 for intensity ranges, bands (0 1 0)–(0 0 0) and (0 2 0)–(0 1 0) of $H_2{}^{16}O$. Wavenumber range corresponding to Table 2 1250–1750 cm^{-1}.

log(S_{min})	log(S_{max})	Offset/%	Offset error/%	No. lines
−26.0	−25.5	4.92	1.70	84
−25.5	−25.0	3.53	0.99	92
−25.0	−24.5	1.00	0.74	91
−24.5	−24.0	0.10	0.54	97
−24.0	−23.5	−0.51	0.29	107
−23.5	−23.0	−0.83	0.24	111
−23.0	−22.5	1.49	0.09	113
−22.5	−22.0	1.40	0.06	114
−22.0	−21.5	1.43	0.06	77
−21.5	−21.0	1.52	0.05	55
−21.0	−20.5	1.64	0.06	54
−20.5	−20.0	1.65	0.05	54
−20.0	−19.5	1.68	0.05	54
−19.5	−19.0	1.63	0.04	55
−19.0	−18.5	1.63	0.06	28

based on experimental data and intercomparison with the *ab initio* results is shown in Fig. 5. Large differences occur increasing from 5% at 10^{-20} to 30% at 10^{-25} cm molecule^{-1}. The EH approach was also used to calculate pure rotational line intensities, also contained in HITRAN2008 and 2012. For these transitions the *ab initio* uncertainties are very small. Fig. 6 shows the differences between *ab initio* and HITRAN2012 for pure rotational transitions which are somewhat smaller than in Fig. 5 with values up to 10% at 10^{-25} cm molecule^{-1}. Since such large differences between *ab initio* and experimental data were not found in cases where the *ab initio* uncertainties are small, it appears that the EH approach has problems extrapolating outside the region for which it fits the experimental data.

The analysis in the ν_2 region yielded also a significant number of $H_2{}^{18}O$ line intensities with high accuracy. The isotopic abundance had to be corrected due to two effects: tap water shows depletion of $H_2{}^{18}O$ which increases with distance from the ocean. From Ref. [64] the depletion was estimated to be about 1%. In case of reversible evaporation of water due to the difference in vapor pressure $H_2{}^{18}O$ is further depleted by another 1% in the vapor phase. A total systematic error of 2% was estimated, combining the pressure, temperature and depletion error. The *ab initio* intensities were scaled by the appropriate abundance and are in HITRAN2012. Fig. 7 shows *ab initio* against experiment for lines with a statistical uncertainty below 5%. Table 4 shows the mean differences (offsets) for different intensity ranges. The difference is about 0.2–0.6% for lines with intensities greater than 10^{-23} cm molecule^{-1} and well within the experimental uncertainties.

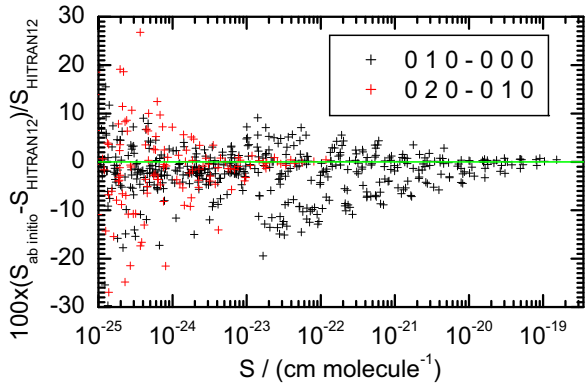

Fig. 5. Percentage intensity difference *ab initio*–HITRAN2012 *vs.* intensity, bands (0 1 0)–(0 0 0) and (0 2 0)–(0 1 0) of $H_2{}^{16}O$. Wavenumber range≥1750 cm^{-1}.

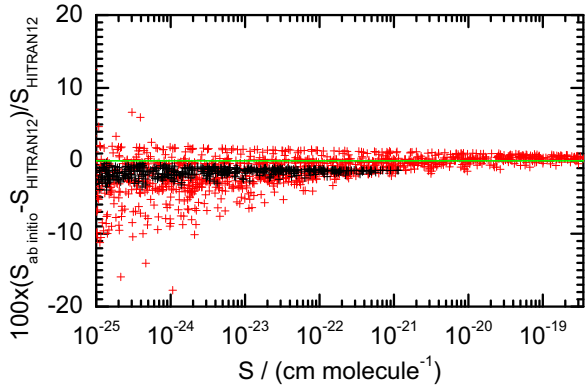

Fig. 6. Percentage *ab initio*–HITRAN2012 *vs.* intensity, bands (0 0 0)–(0 0 0) and (0 1 0)–(0 1 0) of $H_2{}^{16}O$.

4.2. 10,000–11,000 cm^{-1}

As already mentioned these data were analyzed with the speed-dependent Voigt profile but still with single spectrum fits. Fig. 8 shows the percentage differences between the *ab initio* and experimental line intensities together with total uncertainties for lines with statistical uncertainties limited to a maximum of 1%. The total uncertainties used for HITRAN2012 [1] and shown in Fig. 8 were generated by multiplying the statistical uncertainty with the dimensionless standard deviation χ, both resulting from the averaging of line intensities from single spectrum analyses. Furthermore, 1% systematic uncertainty accounting for pressure and temperature uncertainties was added. In the Figure different vibrational bands are color coded. Fig. 9 compares the

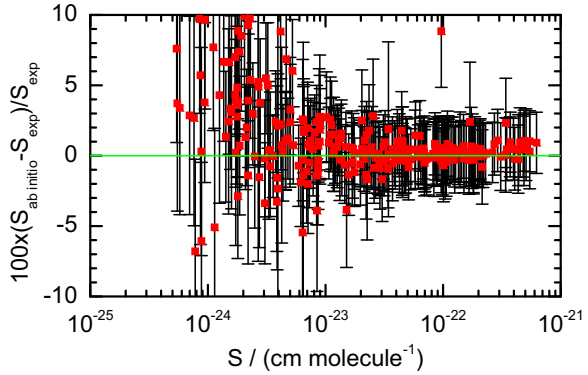

Fig. 7. Percentage *ab initio*–experimental *vs.* intensity, band (0 1 0)–(0 0 0) of $H_2{}^{18}O$. Statistical error limit of experimental data 5%. The error bars indicate the total experimental uncertainties.

Please cite this article as: Birk M, et al. Accurate line intensities for water transitions in the infrared: Comparison of theory and experiment. J Quant Spectrosc Radiat Transfer (2017), http://dx.doi.org/10.1016/j.jqsrt.2017.03.040

Table 4
Percentage *ab initio*–experimental for intensity ranges, bands (0 1 0)–(0 0 0) and (0 2 0)–(0 1 0) of $H_2{}^{18}O$. Statistical error limit of experimental data 5%.

$\log(S_{min})$	$\log(S_{max})$	Offset/%	Offset error/%	No. lines
−24.5	−24.0	3.05	1.52	12
−24.0	−23.5	3.61	0.59	39
−23.5	−23.0	0.85	0.35	52
−23.0	−22.5	0.28	0.17	53
−22.5	−22.0	0.40	0.18	53
−22.0	−21.5	0.23	0.08	44
−21.5	−21.0	0.64	0.14	17

experimental intensities with the *ab initio* ones for individual vibrational bands, sorted by line intensity. Inspecting these comparisons it appears that except for some transitions there seems to be a constant offset between *ab initio* and experimental intensities which differs between vibrational bands. In Table 5 the mean differences for the different vibrational bands are given, ranging from +5.1% to −8.8%. In the averaging individual differences deviating by more than 10% from the mean were removed. The numbers of removed and included lines are given in the last two columns. Furthermore, data were only used in the averaging when the uncertainties for *ab initio* and experimental statistical uncertainties were below the limits indicated in column 5. These differences are certainly not linked to errors in the experiment since systematic errors in line intensities measured simultaneously do not depend on the vibrational states involved; in particular all these bands arise from the vibrational ground state and thus have the same temperature dependence. It should be emphasized that a dependence of systematic errors on the vibrational state with transitions occurring in the same wavenumber range can only be linked to different lower state energies and thus temperature dependence of intensities. In contrast to the *ab initio* calculation the experimental intensity does not do not have systematic dependences on the vibrational band. With the exception of the (3 0 0)–(0 0 0) band, mean differences are within the *ab initio* uncertainties. The behavior of the systematic errors in the *ab initio* calculation affects all rovibrational lines within a vibrational band similarly, probably due to a systematic error in the DMS, mostly covered in the *ab initio* error budget. Another issue is the scatter of data points for different vibrational bands. Inspecting Fig. 9, transitions within the band (3 0 0)–(0 0 0) seem to have a larger scatter. For more quantitative investigation the scatter was calculated, defined as mean absolute deviation from the mean in units of experimental statistical uncertainty. Indeed, the largest value was found for (3 0 0)–(0 0 0). As can be seen for (1 0 0)–(0 0 0) in Section 4.3 there is also a larger scatter. This scatter turns out to be a systematic error of the *ab initio* calculation when the differences are plotted *vs.* wavenumber or lower state energy with color coding of different ΔK_a and ΔJ (Figs. 16 and 17). In the present case a similar investigation did not reveal systematic behavior due to the lack of a sufficient number of high precision data.

Fig. 8 shows the *ab initio* uncertainties for the band with the largest number of lines. There are plenty of lines where the *ab initio* uncertainty is huge. However, for most of these lines the actual differences are small. On the other hand, there are some lines where *ab initio* uncertainties are small and differences large, see, for example, some lines in the range #20 to #40 in the top panel of Fig. 9.

The reason appears to be incorrect identification of resonant rovibrational states. This becomes clear by inspection of Table 6. The *ab initio* predicted resonance has a large *ab initio* uncertainty because the mixing of states cannot be predicted precisely. However, the actual difference for $J'' = 6$ is small despite the huge *ab initio* error. It appears that the PES used to calculate the listed intensity for the predicted resonance at $J'' = 6$ is actually performing well but the secondary PES is not. In particular we note that stability analysis was performed with wavefunctions generated using an accurate, spectroscopically-determined PES and an *ab initio* PES. Recent studies on CO_2 [49] and HDO [65] both found that use of an *ab initio* PES did not give the best results and instead used two, distinct empirical PESs.

4.3. 1850–2280 cm^{-1} and 2390–4000 cm^{-1}

The measurements in this spectral region were analyzed applying a speed-dependent Voigt profile in the HTP-implementation [36–40] including Rosenkranz line-mixing. For intercomparison the main isotopologue *ab initio* intensities were scaled applying a factor of 0.9976 corresponding to the natural abundance of $H_2{}^{16}O$. Fig. 10 shows the relative differences between *ab initio* and experimental line intensities of $H_2{}^{16}O$ together with the total experimental error. For the plot the data were limited to intensities with errors less than 1%. For clarity the differences were grouped according to change of vibrational quantum numbers. Figs. 11 and 12 give the differences for the individual vibrational bands sorted by line intensity and the *ab initio* uncertainties are given. Fig. 11 shows numerous lines of the ν_1

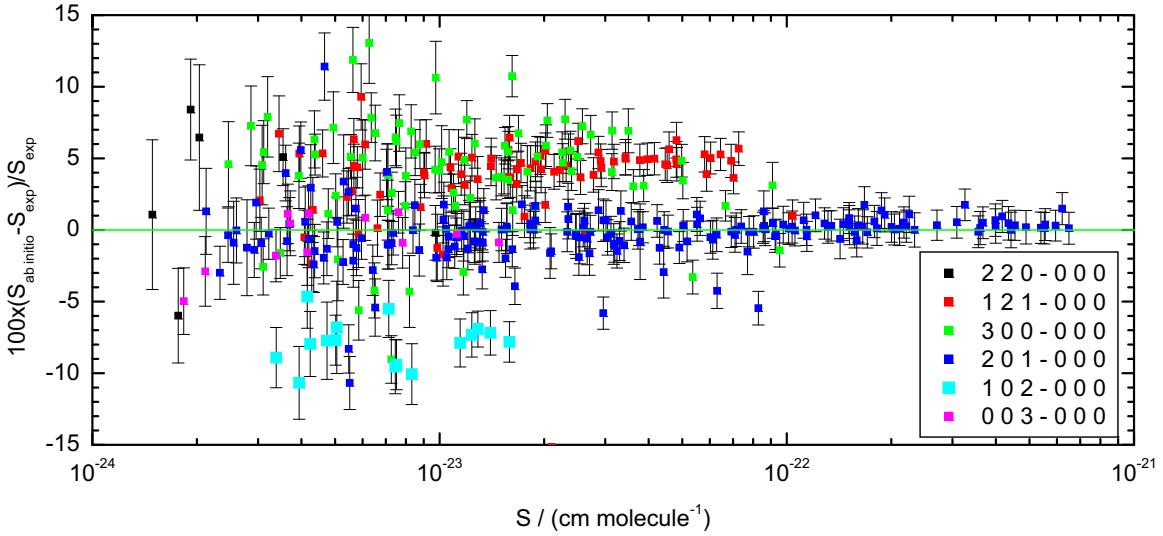

Fig. 8. Percentage *ab initio*–experimental *vs.* intensity, bands in 1 μm region of $H_2{}^{16}O$. Statistical error limit of experimental data 1%. The error bars indicate the total experimental uncertainties. (For interpretation of the references to color in this figure, the reader is referred to the web version of this artic.

Please cite this article as: Birk M, et al. Accurate line intensities for water transitions in the infrared: Comparison of theory and experiment. J Quant Spectrosc Radiat Transfer (2017), http://dx.doi.org/10.1016/j.jqsrt.2017.03.040

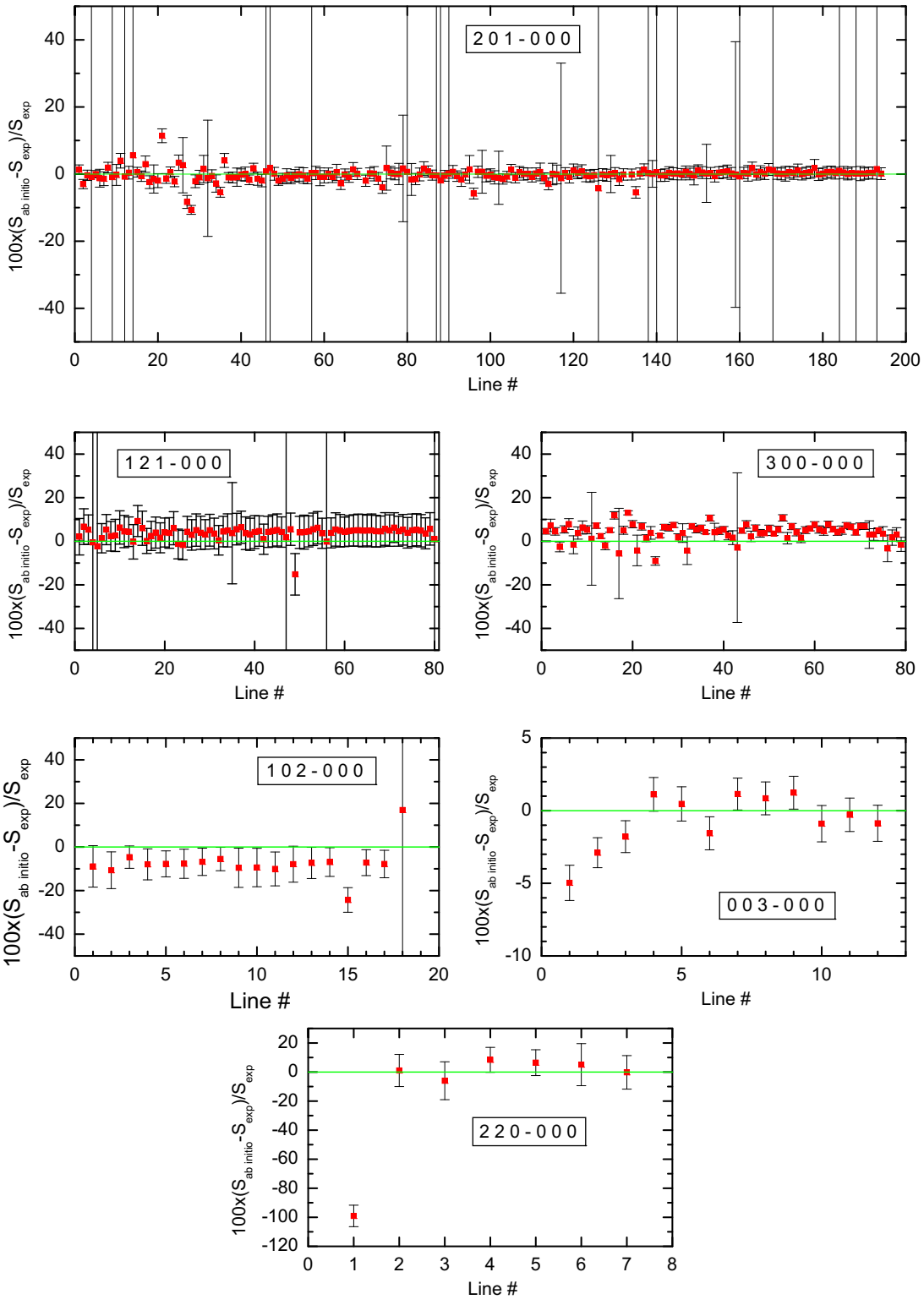

Fig. 9. Percentage *ab initio*–experimental *vs*. line number, sorted by intensity for the 3ν polyad stretching bands of $H_2{}^{16}O$. Statistical error limit of experimental data 1%. The error bars indicate the *ab initio* uncertainties. There are a significant number of transitions with large *ab initio* uncertainties but small actual differences and vice versa. From the top: (a) (2 0 1)–(0 0 0); (b) (1 2 1)–(0 0 0); (c) (3 0 0)–(0 0 0); (d) (1 0 2)–(0 0 0); (e) (0 0 3)–(0 0 0); (f) (2 2 0)–(0 0 0). (For interpretation of the references to color in this figure, the reader is referred to the web version of this article).

vibrational band where differences exceed the *ab initio* uncertainties, in contrast to the previously discussed regions. Similar to experimental regions 1 and 2 there seem to be constant offsets and scatter level specific to vibrational bands.

Table 7 gives the mean differences for the various vibrational bands. For the average calculations intensities with specified *ab initio* and experimental uncertainties >10% and 1%, respectively, were excluded. In addition to the mean differences the scatter level (as previously defined) and the number of lines included and excluded from the calculations are given. The mean deviations range from −2.2% for the ν_1 fundamental band to +0.34% for the ν_2 hot band. In particular, intensities belonging to vibrational bands with change of the ν_1

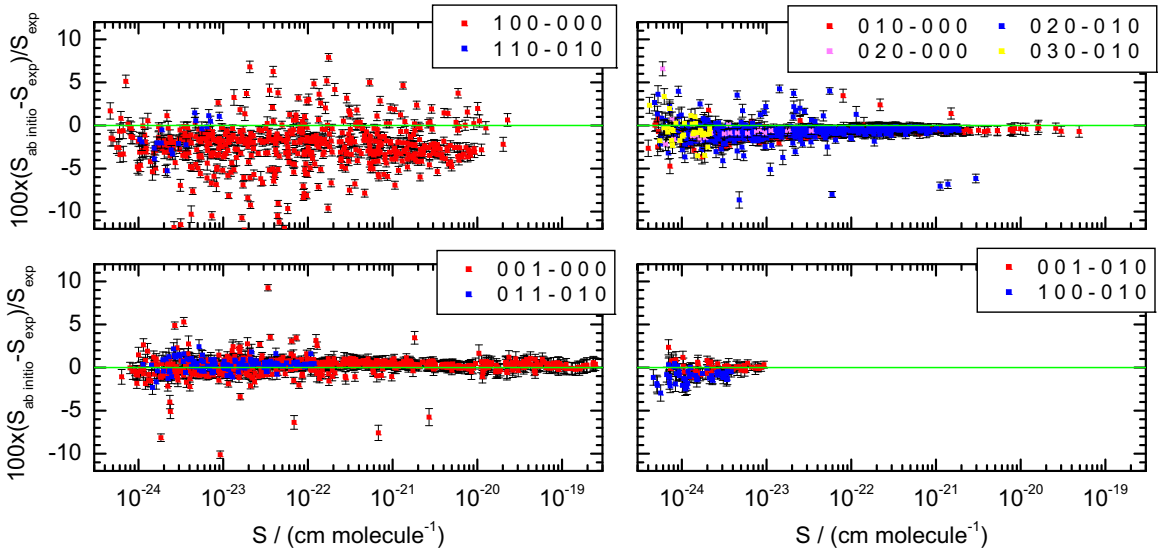

Fig. 10. Percentage *ab initio*–experimental *vs.* intensity, bands in 1850–2280 cm^{-1} and 2390–4000 cm^{-1} region of $H_2{}^{16}O$. The error limit of the experimental data is 1%.

Table 5
Offset and scatter for bands in the 1 μm region.

Band	Offset/%	Offset error/%	Scatter	*Ab initio*/ DLR uncert limit/%	No included	No removed
121 000	4.2	0.2	1.6	10/1	73	1
201 000	−0.4	0.2	1.7	5/1	160	2
300 000	5.1	0.4	2.0	3/1	64	0
102 000	−8.8	1.0	1.4	15/1	17	0
003 000	−0.7	0.5	1.0	2/1	12	0
220 000	2.5	2.1	1.2	15/5	6	1

Table 6
Subband $J+1_{0,J+1}-J_{0,J}$ in (2 0 1)–(0 0 0) band. Predicted resonance at $J=6$ and actual resonance at $J=11$.

J	$\sigma(S_{abinitio})$/%	$(S_{abinitio}-S_{exp})$/%
0	4.0	0.0
2	1.8	0.3
4	1.7	0.1
6	5630.3	0.3
7	8.7	0.2
8	1.6	−0.6
9	1.5	−0.8
11	1.4	−1.7

vibrational quantum number show an obviously larger scatter than the other vibrational bands. This finding matches the large scatter in the $3\nu_1$ band discussed in the preceding section. The systematic nature of this scatter is detailed in Section 4.5.

As a result of the analysis also intensities for $H_2{}^{18}O$ and $H_2{}^{17}O$ were obtained. These intensities were corrected for isotopologue depletion as described for $H_2{}^{18}O$ intensities of experimental region 1. For $H_2{}^{17}O$ a correction of 1% was applied depicting the fractionation factor difference of $H_2{}^{17}O$ and $H_2{}^{18}O$ [66]. The relative difference of *ab initio* intensities and experimental values are plotted *versus* the line intensity in Figs. 13 and 14. The mean deviation (offset) and scatter specific to vibrational bands are given in Tables 8 and 9. In the case of $H_2{}^{18}O$, the constant offset and large scatter for the ν_1 band seen for the main isotopologue is again visible. For $H_2{}^{17}O$ the offsets are monotonically smaller (about 2–3%) than for $H_2{}^{16}O$ and $H_2{}^{18}O$. From theory it is expected that *ab initio* intensities for the same band for different isotopologues should exhibit the same offsets. The reason for the differences in $H_2{}^{17}O$ intensities may be linked to the accuracy of the ^{17}O isotopic abundance. The *ab initio* values included in HITRAN12 use the ^{17}O isotopic abundance 0.0373% given in the HITRAN database Supplement files. The abundance given by NIST[1] is 0.038(1)% which is 1.9% larger. Scaling the HITRAN data to the NIST means that the best-determined band of $H_2{}^{17}O$ has an offset of +0.7% which is in agreement with $H_2{}^{16}O$. For high accuracy work, the accuracy of the $H_2{}^{17}O$ isotopic abundance is rather low since the HITRAN and NIST value are within the 1σ uncertainty of NIST.

4.4. 4190–4340 cm^{-1}

Fig. 15 and Table 10 show the relative differences of $H_2{}^{16}O$ *ab initio* intensities to experimental values for the spectral range 4190–4340 cm^{-1} in the same way as for experimental regions 1, 2 and 3 above. Since no detailed error propagation calculations as for region 3 were performed, an experimental error of 0.4%, corresponding to typical experimental errors of intensities from region 3, was adopted in addition to the statistical error of the multispectrum fit. These errors are shown in Fig. 15 and used for the calculation of mean differences and scatter shown in Table 10. Interestingly, the offsets obtained do not match the ones from region 3 although the analysis procedure applied was identical. This issue is discussed in detail in the following section.

4.5. Rotational quantum number dependence of differences

In the last sections the differences between theoretical and experimental line intensities were investigated by plotting/averaging with respect to line intensities. Fig. 16 shows the percentage differences *ab initio*– experimental *versus* wavenumber from the combined results of experimental regions 3 and 4. Color coding is supplied for the different ΔK_a values of the transitions. While many transitions show differences below 2%, there are also systematic differences of up to 12% which show not only a clear wavenumber dependence but also clear dependence on ΔK_a. This systematic behavior becomes even clearer when plotting color-coded *P*-, *Q*-, and *R*-branches for a given

[1] [https://www.nist.gov/pml/atomic-weights-and-isotopic-compositions-relative-atomic-masses]

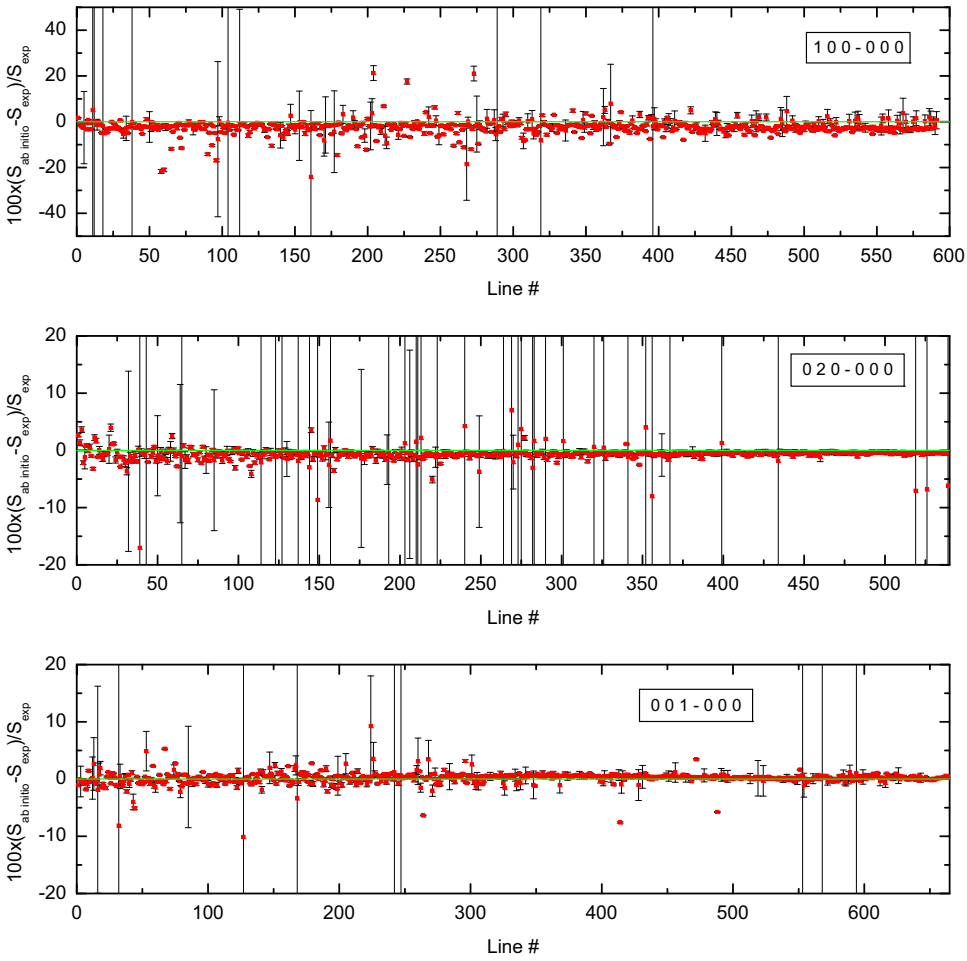

Fig. 11. Percentage *ab initio*-experimental by line number, sorted by intensity, for selected bands of $H_2{}^{16}O$. The statistical error limit of the experimental data is 1%. The error bars indicate the *ab initio* uncertainties.

ΔK_a *versus* the lower state energy, E_i, as shown in Fig. 17. The large scatter in Table 7 is likely to be linked to these differences.

Wavenumber and ΔK_a dependence as for the (1 0 0)–(0 0 0) band are shown for the (0 0 1)–(0 0 0), (0 1 0)–(0 0 0), and (0 2 0)–(0 0 0) bands in Figs. 18–20. There are systematic differences, mainly between different ΔK_a subbands, for (0 0 1)–(0 0 0) but much smaller than for the (1 0 0)–(0 0 0) band. Generally, the differences are within $\pm 2\%$. For the (0 1 0)–(0 0 0) band there are differences between different ΔK_a subbands and as a function of wavenumber within a given ΔK_a. The effects are rather small and within 2%. It was investigated whether the differences in the mean of the regions 1 and 3 (see Tables 2 and 7) is linked to this systematic wavenumber dependence. The differences in Table 2 were nearly constant in the intensity range 2×10^{-23}–2×10^{-22} cm molecule^{-1}. Fig. 21 plots the differences within this intensity range against wavenumber. Indeed, at 1750 cm^{-1} and at 1850 cm^{-1} in Fig. 19 the differences are about the same. In Fig. 20 the differences for (0 2 0)–(0 0 0) show mainly a wavenumber dependence of up to 2%. In general, the wavenumber dependence for a given ΔK_a and ΔJ may be a dependent on the J quantum number. It should be noted that in Figs. 16 and 18 the consistency of the data for lines with ΔK_a=+3 or +2, respectively, coming from regions 3 and 4 can be clearly seen, indicating the absence of systematic errors of the two completely independent experiments and thus underlining the high quality of the present data.

The clear ΔK_a dependence of the comparison shown by the ν_1 band and the suggestion that it might be present in other stretching bands implies that there is a residual issue with the theoretical calculations. At present it is unclear what is causing this problem. A previous analysis of *ab initio* calculations aimed precisely at identifying ΔK_a-dependent issues in the spectrum of $H_2{}^{16}O$ found no such issues [67]. However, this study only considered pure rotational bands and it is clear that more work is required to understand this behavior for bands involving stretching excitation.

5. Summary of comparison

The overall agreement between experimental and *ab initio* H_2O line intensities is excellent and, except for many transitions with change in ν_1 quanta, within the larger of the *ab initio* and experimental uncertainties. There are several vibrational bands with an average agreement better than 1%, among those are the fundamentals ν_2 and ν_3 for $H_2{}^{16}O$ and $H_2{}^{18}O$. Aside from resonances there appears to be a constant offset for a given vibrational band when displaying differences *vs.* intensities. In the same plots, bands with a change of ν_1 quanta show a larger scatter of the differences. Investigating the differences as function of wavenumber, ΔK_a, and ΔJ reveals systematic dependences. These differences are ± 1% for ν_3, 0% to −2% for ν_2, and −13% to +5% for ν_1. Local resonances in *ab initio* calculations may be misplaced due to wrong energy term values of resonating states leading to significant (>10%) differences for individual lines.

$H_2{}^{16}O$ fundamental bands:

- ν_1 shows rather large offset of −2.2%.
- ν_2 shows an offset of −0.85% for the multispectrum fit results above 1800 cm^{-1}. The results between 1250 and 1750 cm^{-1} are 0.7% for lines around 10^{-22} cm molecule^{-1} and 2.1 % for the

Please cite this article as: Birk M, et al. Accurate line intensities for water transitions in the infrared: Comparison of theory and experiment. J Quant Spectrosc Radiat Transfer (2017), http://dx.doi.org/10.1016/j.jqsrt.2017.03.040

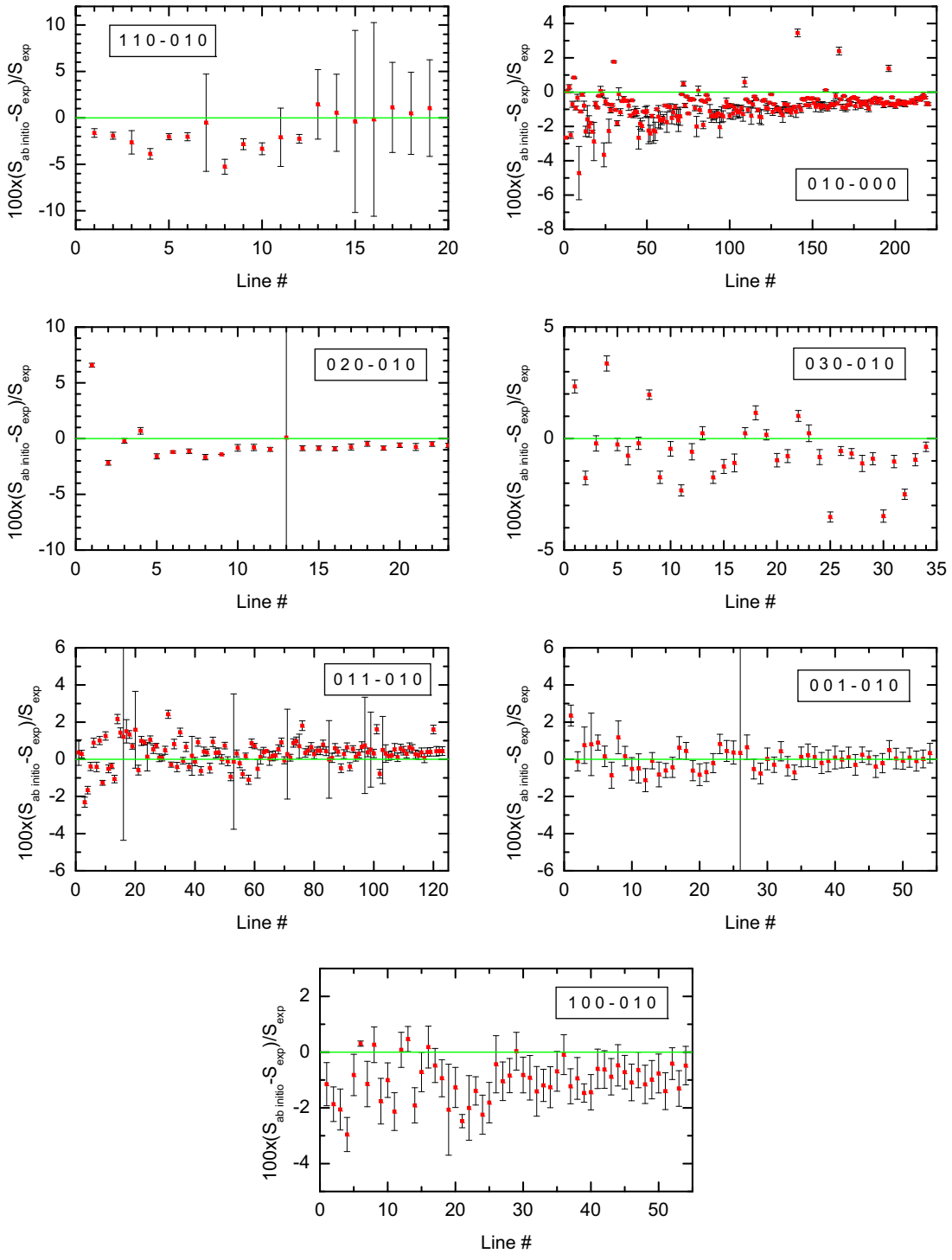

Fig. 12. Percentage *ab initio*–experimental by line number, sorted by intensity, for selected bands of $H_2{}^{16}O$. The statistical error limit of the experimental data is 1%. The error bars indicate the *ab initio* uncertainties.

strongest lines. The effective Hamiltonian approach showed differences from 1.4% to 1.6%. The reason for the discrepancy of the old and newer results on the order of 2% may be attributed to the quantum number or wavenumber dependence as described above. Furthermore, a systematic error caused by the use of the Voigt profile in the analysis instead of the speed-dependent Voigt may be present. The ν_2 old analysis is the only case where the offset is intensity dependent. For the strong lines the optical depth in the experimental spectra is on average larger than for the weaker lines. A wrong line model will cause optical-depth-dependent line intensity errors. Furthermore, the offset increases for very weak lines as can be seen in Fig. 1 and Table 2. The reason is unclear but certainly an experimental error. A re-analysis of the ν_2 data with the multispectrum fitting tool may clarify these issues. Still these results are a considerable improvement over the previous results used in HITRAN2004 [68] where the differences *ab initio*–HITRAN2004 change continuously from +4% for strong lines to −2% for weak lines with a larger scatter.

- The ν_3 band shows excellent agreement with only 0.2% offset.

Please cite this article as: Birk M, et al. Accurate line intensities for water transitions in the infrared: Comparison of theory and experiment. J Quant Spectrosc Radiat Transfer (2017), http://dx.doi.org/10.1016/j.jqsrt.2017.03.040

Table 7
Offset and scatter for $H_2{}^{16}O$ bands in the 1850–2280 cm^{-1} and 2390–4000 cm^{-1} spectral ranges. The *ab initio* and DLR uncertainty limits were fixed at 10% and 1%, respectively, for all bands.

Band	Offset/%	Offset error/%	Scatter	No included	No removed
100 000	−2.2	1.9	2.9	425	67
110 010	−1.4	1.9	2.3	19	1
010 000	−0.85	0.80	0.96	220	0
020 010	−0.54	1.7	1.2	22	1
020 000	−0.65	0.80	0.95	498	41
030 010	−0.60	1.4	1.4	34	0
001 000	+0.18	0.91	1.0	652	13
011 010	+0.34	0.70	0.78	123	0
100 010	−1.0	0.73	0.78	54	0
001 010	+0.01	0.60	0.72	53	1

Overtones from ground state $H_2{}^{16}O$:

- ν_1 (3 0 0)–(0 0 0) shows rather large offset (5.1%) and large scatter
- ν_2 (0 2 0)–(0 0 0) shows excellent agreement with only 0.7% difference
- ν_3 (0 0 3)–(0 0 0) shows excellent agreement with only 0.7% difference

Combination bands from ground state $H_2{}^{16}O$:

- (1 2 1), (2 0 1), (1 0 2), (2 2 0): Offsets between 0.4% and 8.8%

Hot and difference bands originating from (0 1 0) $H_2{}^{16}O$:

- Upper vibrational state: (1 1 0), (0 2 0), (0 3 0), (0 1 1), (1 0 0), (0 0 1). Offsets between 0.0% and 1.4%.

$H_2{}^{18}O$ fundamental bands:

- ν_1 shows rather large offset (−3.1%) and large scatter.
- ν_2 in the old analysis based on Voigt profile the offset was +0.5% while it is −1.0% in the new analysis. The same discrepancy was found for $H_2{}^{16}O$ for weaker lines (see above).
- ν_3 shows excellent agreement with no difference.

Overtone from ground state $H_2{}^{18}O$:

- ν_2 (0 2 0)–(0 0 0) shows excellent agreement with only 0.7% difference.

The systematic line intensity dependent variation is likely caused by the lack of vibrational narrowing in the line model used for analysis and shows the usefulness of the *ab initio* data in assessing experimental data.

$H_2{}^{17}O$ fundamental bands:

- ν_1 shows rather large offset (−4.8%) and large scatter.
- ν_2 shows rather large offset (−3.6%) (only new analysis).
- ν_3 shows moderate offset (−2.2%).

The larger offset found for $H_2{}^{17}O$ is largely caused by assumed values for the natural abundance of $H_2{}^{17}O$.

One issue that has not been discussed thus far is the issue of representation of the *ab initio* DMS. The standard procedure is to compute dipoles at a grid of points and then fit them to an appropriate functional form. Choice of this form is important [69] and it is well-known that use of too few *ab initio* points can lead to artificial features in the fitted surface [14,70]. Recent studies of the high stretching overtones which absorb weakly in the near ultraviolet [62] have shown very strong sensitivity to the underlying fit. It would

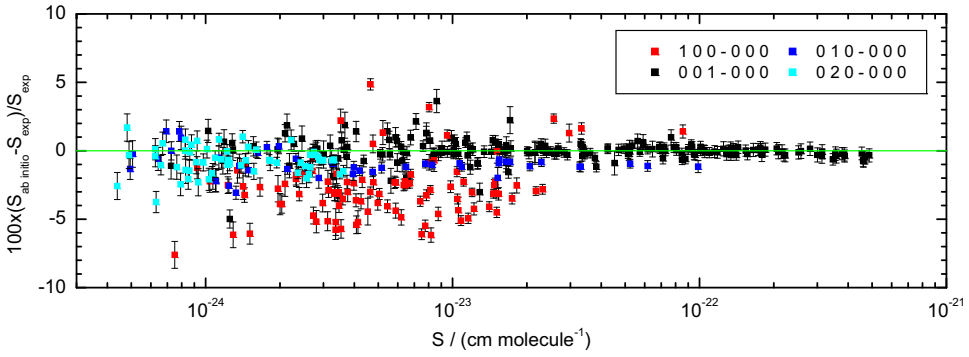

Fig. 13. Percentage *ab initio*–experimental *vs.* intensity, bands in 1850–2280 cm^{-1} and 2390–4000 cm^{-1} region of $H_2{}^{18}O$. The error limit of the experimental data is 1%.

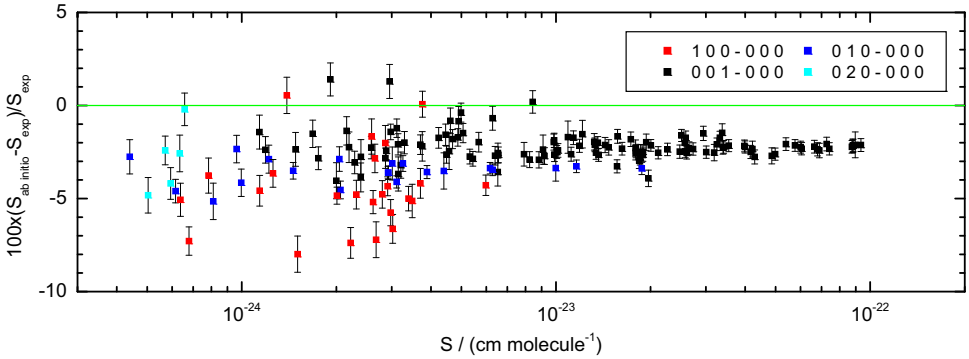

Fig. 14. Percentage *ab initio*–experimental *vs.* intensity, bands in 1850–2280 cm^{-1} and 2390–4000 cm^{-1} region of $H_2{}^{17}O$. The error limit of the experimental data is 1%.

Please cite this article as: Birk M, et al. Accurate line intensities for water transitions in the infrared: Comparison of theory and experiment. J Quant Spectrosc Radiat Transfer (2017), http://dx.doi.org/10.1016/j.jqsrt.2017.03.040

Table 8
Offset and scatter for $H_2{}^{18}O$ bands in the 1850–2280 cm^{-1} and 2390–4000 cm^{-1} spectral ranges. The *ab initio* and DLR uncertainty limits were fixed at 10% and 1%, respectively, for all bands.

Band	Offset/%	Offset error/%	Scatter	No included	No removed
100 000	−3.1	1.8	2.3	97	4
010 000	−1.0	0.88	1.1	45	0
020 000	−0.73	1.0	1.2	58	0
001 000	−0.02	0.82	0.92	199	0

Table 9
Offset and scatter for $H_2{}^{17}O$ bands in the 1850–2280 cm^{-1} and 2390–4000 cm^{-1} spectral ranges. The *ab initio* and DLR uncertainty limits were fixed at 10% and 1%, respectively, for all bands.

Band	Offset/%	Offset error/%	Scatter	No included	No removed
100 000	−4.8	2.6	2.1	25	0
010 000	−3.6	0.67	0.80	21	0
020 000	−2.8	1.8	1.5	5	0
001 000	−2.2	0.78	0.97	120	1

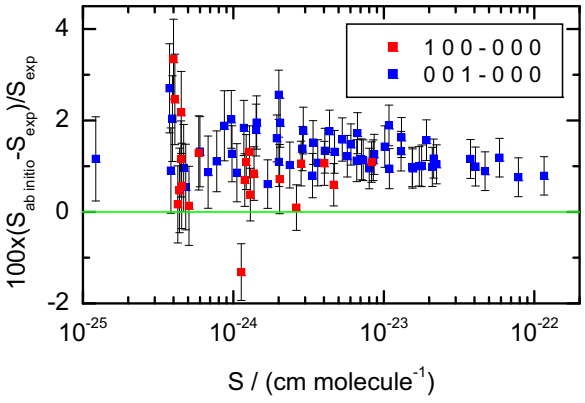

Fig. 15. Percentage intensity difference *ab initio*–experimental *vs.* intensity, bands in 4190–4340 cm^{-1} region of $H_2{}^{16}O$. The error limit of the experimental data is 1%.

Table 10
Offset and scatter for $H_2{}^{16}O$ bands in the 4190–4340 cm^{-1} spectral range. The *ab initio* and DLR uncertainty limits were fixed at 10% and 1%, respectively, for all bands.

Band	Offset/%	Offset error/%	Scatter	No included	No removed
100 000	+0.92	0.21	0.89	21	3
001 000	+1.3	0.06	0.66	59	5

seem likely that low-lying bands may also be affected by this. Lodi et al. [16] used 2626 geometries when computing their *ab initio* dipoles. It would appear that to get a more accurate DMS a significant increase in this number will be needed, as well as an improvement of the *ab initio* treatment employed.

6. Conclusion

Water line intensity data in the mid and near infrared region were measured at DLR and predicted theoretically. The only experimental input for the *ab initio* calculations are the rovibrational energy levels used to derive the PES. The average agreement between experimental and *ab initio* H_2O line intensities is excellent and, except for many transitions with change in ν_1 quanta, within the larger of the *ab initio* and experimental uncertainties. There are several vibrational bands with an agreement better than 1%, among those the fundamentals ν_2 and ν_3 for $H_2{}^{16}O$ and $H_2{}^{18}O$. An important finding of this work is that for an individual vibrational band an intensity independent offset appears in graphical representations of differences between experiment and theory *vs.* intensity. This holds only in absence of local resonances. This information can be used to

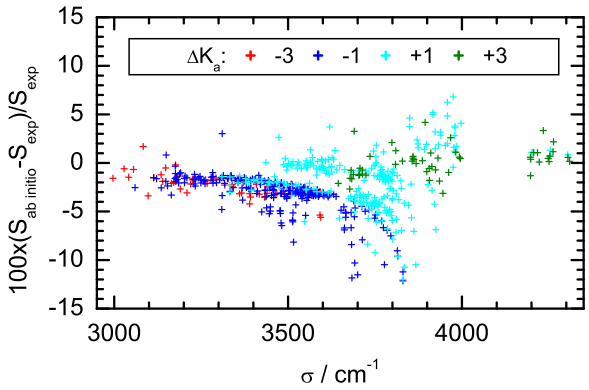

Fig. 16. Percentage intensity difference *ab initio*-experimental against wavenumber for the (1 0 0)–(0 0 0) band, red: $\Delta K_a = -3$, blue: $\Delta K_a = -1$, cyan: $\Delta K_a = +1$, green: $\Delta K_a = +3$. The statistical error limits of the experimental data is 1%. In the gap 4000–4190 cm^{-1} data were not analyzed due to the requirements of the individual projects (see Table 1). (For interpretation of the references to color in this figure legend, the reader is referred to the web version of this article).

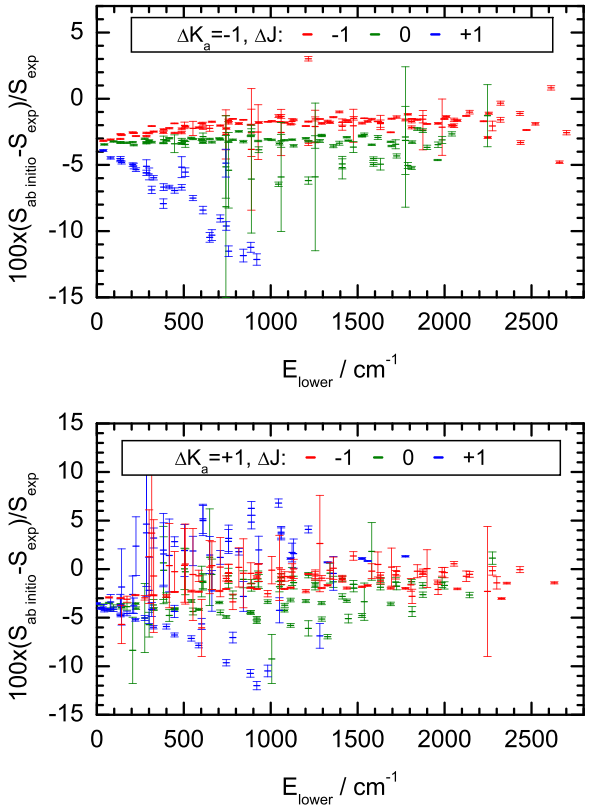

Fig. 17. Percentage intensity difference *ab initio*–experimental against lower state energy for the (1 0 0)–(0 0 0) band. Upper panel: subband $\Delta K_a = -1$; lower panel: subband $\Delta K_a = +1$. Red: $\Delta J = -1$, green: $\Delta J = 0$, blue: $\Delta J = +1$. The statistical error limit on the experimental data is 1%. Error bars refer to the *ab initio* uncertainties. (For interpretation of the references to color in this figure legend, the reader is referred to the web version of this article).

Please cite this article as: Birk M, et al. Accurate line intensities for water transitions in the infrared: Comparison of theory and experiment. J Quant Spectrosc Radiat Transfer (2017), http://dx.doi.org/10.1016/j.jqsrt.2017.03.040

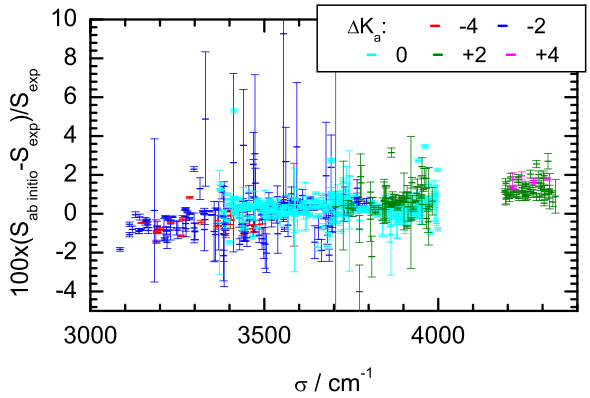

Fig. 18. Percentage intensity difference *ab initio*–experimental *vs.* wavenumber for the (0 0 1)–(0 0 0) band, red: $\Delta K_a = -4$, blue: $\Delta K_a = -2$, cyan: $\Delta K_a = 0$, grey: $\Delta K_a = +2$, purple: $\Delta K_a = +4$. Statistical error limit of experimental data 1%. In the gap 4000–4190 cm^{-1} data were not analyzed due to the requirements of the individual projects (see Table 1). (For interpretation of the references to color in this figure legend, the reader is referred to the web version of this article).

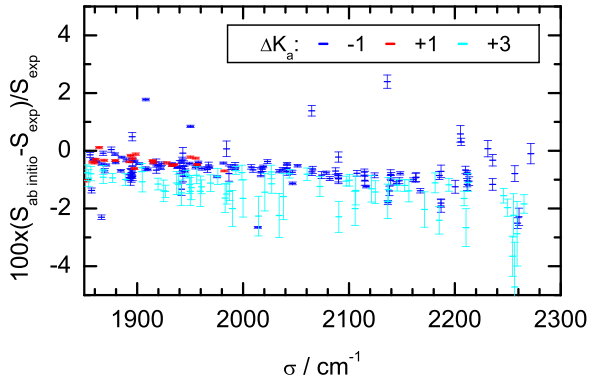

Fig. 19. Percentage intensity difference *ab initio*–experimental *vs.* wavenumber for the (0 1 0)–(0 0 0) band, red: $\Delta K_a = -1$, blue: $\Delta K_a = +1$, cyan: $\Delta K_a = +3$. Statistical error limit of experimental data 1%. (For interpretation of the references to color in this figure legend, the reader is referred to the web version of this article).

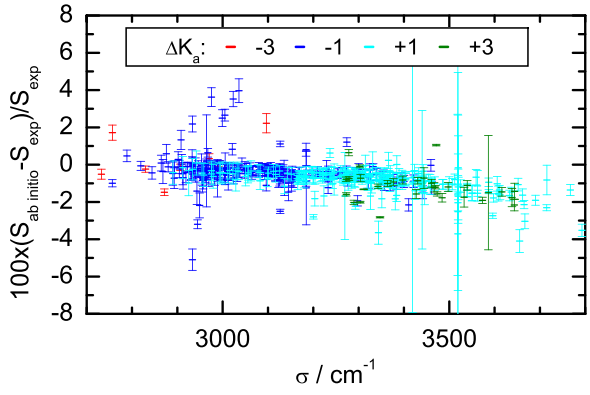

Fig. 20. Percentage intensity difference ab *ab initio*–experimental *vs.* wavenumber for the (0 2 0)–(0 0 0) band, red: $\Delta K_a = -3$, blue: $\Delta K_a = -1$, cyan: $\Delta K_a = +1$, green: $\Delta K_a = +3$. Statistical error limit of experimental data 1%. (For interpretation of the references to color in this figure legend, the reader is referred to the web version of this article).

validate experiment as well as theory. For example, the error in the Voigt analysis in the ν_2 becomes clear from the intensity dependent offset. On the other hand a large offset shows the limitations of the DMS. The constant offset can also be used to predict weak line intensities where experimental data are unavailable by scaling *ab initio*

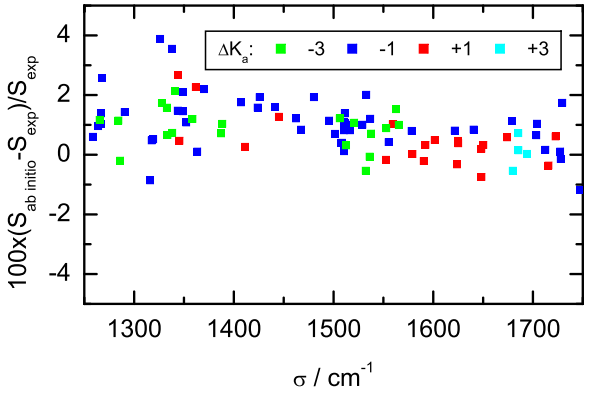

Fig. 21. Percentage intensity difference *ab initio*–experimental *vs.* wavenumber for the (0 1 0)–(0 0 0) band, green: $\Delta K_a = -3$, blue: $\Delta K_a = -1$, red: $\Delta K_a = +1$, cyan: $\Delta K_a = +3$. Line intensity boundaries 2×10^{-23}–2×10^{-22} cm molecule^{-1} to avoid error from Voigt. Statistical error limit of experimental data 1%. (For interpretation of the references to color in this figure legend, the reader is referred to the web version of this article).

values. It was found that, besides transitions with changes in the ν_1 quantum number, the systematic differences to the *ab initio* values were, on average, below the specified *ab initio* uncertainties. Thus, experimental data for spectral regions not shown in this work could be validated using the *ab initio* data.

For some bands, larger differences and a large scatter occur for bands with a change of ν_1 quanta. Investigating the differences as function of wavenumber, ΔK_a, and ΔJ reveals systematic dependences. These differences are, to a lesser extent, also visible for the ν_2 and ν_3 fundamentals. The corresponding problems in the *ab initio* calculations need to be addressed.

The prediction of local resonances requires sufficiently accurate energy levels for the resonating states. This accuracy is not sufficient for transitions in the 1 μm region. Certainly the experimentally found intensity perturbations can be used to improve the energy levels. The larger differences for the $H_2{}^{17}O$ need more experimental data for intercomparison.

The most outstanding issue is that the excellent agreement between experiment and theory within the error margins for most transitions shows the maturity of both approaches and both can benefit from each other. The DLR experimental approach aims for small and characterized uncertainties by using dedicated hardware and analysis tools together with procedures for validated data product accuracy. The *ab initio* calculation also required many years of experience and iterations. The present study provides important input which will aid further improvements in the development of high-accuracy *ab initio* models.

Acknowledgements

The DLR team acknowledges BMBF support in the frame of the HGF- Vernetzungsfonds “Generierung und Validierung von Datenprodukten aus ENVISAT”-'Messungen sowie deren Nutzung zur Erforschung der oberen Troposphaere und Stratosphaere', DFG support under contract numbers BI 834/5-1 and -2, ESA support within SEOM-IAS (ESA/AO/1-7566/13/I-BG), and support by the WDC-RSAT at DLR. This work was supported by NERC under various grants (NE/F01967X/1, NE/J010316/1 and NE/N001508/1). AAK and NFZ acknowledge support by State Project IAP RAS No. 0035-2014-009.

Appendix A. Supplementary data

Supplementary data associated with this article can be found in the online version at http://dx.doi.org/10.1016/j.jqsrt.2017.03.040.

References

[1] Rothman LS, Gordon IE, Babikov Y, Barbe A, Benner DC, Bernath PF, et al. The HITRAN 2012 molecular spectroscopic database. J Quant Spectrosc Radiat Transf 2013;130:4–50. http://dx.doi.org/10.1016/jqsrt.2013.07.002.

[2] Tennyson J, Bernath PF, Brown LR, Campargue A, Carleer MR, Császár AG, et al. IUPAC critical evaluation of the rotational-vibrational spectra of water vapor. Part I. Energy levels and transition wavenumbers for $H_2{}^{17}O$ and $H_2{}^{18}O$. J Quant Spectrosc Radiat Transf 2009;110:573–596. http://dx.doi.org/10.1016/j.jqsrt.2009.02.014.

[3] Tennyson J, Bernath PF, Brown LR, Campargue A, Carleer MR, Császár AG, et al. IUPAC critical evaluation of the rotational-vibrational spectra of water vapor. Part II. Energy levels and transition wavenumbers for $HD^{16}O$, $HD^{17}O$, and $HD^{18}O$. J Quant Spectrosc Radiat Transf 2010;111:2160–2184. http://dx.doi.org/10.1016/j.jqsrt.2010.06.012.

[4] Tennyson J, Bernath PF, Brown LR, Campargue A, Carleer MR, Császár AG, et al. IUPAC critical evaluation of the rotational-vibrational spectra of water vapor. Part III. Energy levels and transition wavenumbers for $H_2{}^{16}O$. J Quant Spectrosc Radiat Transf 2013;117:29–80. http://dx.doi.org/10.1016/j.jqsrt.2012.10.002.

[5] Tennyson J, Bernath PF, Brown LR, Campargue A, Császár AG, Daumont L, et al. A database of water transitions from experiment and theory (IUPAC technical report). Pure Appl Chem 2014;86:71–83. http://dx.doi.org/10.1515/pac-2014-5012.

[6] Tennyson J, Bernath PF, Brown LR, Campargue A, Császár AG, Daumont L, et al. IUPAC critical evaluation of the rotational-vibrational spectra of water vapor. Part IV. Energy levels and transition wavenumbers for $D_2{}^{16}O$, $D_2{}^{17}O$ and $D_2{}^{18}O$. J Quant Spectrosc Radiat Transf 2014;142:93–108. http://dx.doi.org/10.1016/j.jqsrt.2014.03.019.

[7] Furtenbacher T, Dénes N, Tennyson J, Naumenko OV, Polyansky OL, Zobov NF, et al. Update of the IUPAC database of water energy levels. J Quant Spectrosc Radiat Transf 2017 (In preparation).

[8] Fischer H, Birk M, Blom C, Carli B, Carlotti M, von Clarmann T, et al. MIPAS: an instrument for atmospheric and climate research. Atmos Chem Phys 2008 (8):2151–2188.

[9] Lisak D, Hodges JT. Low-uncertainty H2O line intensities for the 930-nm region. J Mol Spectrosc 2008;249:6–13. http://dx.doi.org/10.1016/j.jms.2007.12.007.

[10] Hodges JT, Lisak D, Lavrentieva N, Bykov A, Sinitsa L, Tennyson J, et al. Comparison between theoretical calculations and high-resolution measurements of pressure-broadening for water vapor spectra near 935 nm. J Mol Spectrosc 2008;249:86–94.

[11] Lisak D, Havey DK, Hodges JT. Spectroscopic line parameters of water vapor for rotation-vibration transitions near 7180 cm(-1). Phys Rev A 2009;79:052507. http://dx.doi.org/10.1103/PhysRevA.79.052507.

[12] Birk M, Wagner G. Voigt profile introduces optical depth dependent systematic errors – detected in high resolution laboratory spectra of water. J Quant Spectrosc Radiat Transf 2016;170:159–168. http://dx.doi.org/10.1016/j.jqsrt.2015.11.008.

[13] Gabriel W, Reinsch EA, Rosmus P, Carter S, Handy NC. Theoretical integrated vibrational band intensities of water-vapor. J Chem Phys 1993;99:897–900. http://dx.doi.org/10.1063/1.465354.

[14] Schwenke DW, Partridge H. Convergence testing of the analytic representation of an ab initio dipole moment function for water: Improved fitting yields improved intensities. J Chem Phys 2000;113:6592–6597.

[15] Lodi L, Tolchenov RN, Tennyson J, Lynas-Gray AE, Shirin SV, Zobov NF, et al. A new ab initio ground-state dipole moment surface for the water molecule. J Chem Phys 2008;128:044304.

[16] Lodi L, Tennyson J, Polyansky OL. A global, high accuracy ab initio dipole moment surface for the electronic ground state of the water molecule. J Chem Phys 2011;135:034113. http://dx.doi.org/10.1063/1.3604934.

[17] Lodi L, Tennyson J. Line lists for $H_2{}^{18}O$ and $H_2{}^{17}O$ based on empirically-adjusted line positions and ab initio intensities. J Quant Spectrosc Radiat Transf 2012;113:850–858. http://dx.doi.org/10.1016/j.jqsrt.2012.02.023.

[18] Regalia L, Oudot C, Mikhailenko S, Wang L, Thomas X, Jenouvrier A, et al. Water vapor line parameters from 6450 to 9400 cm^{-1}. J Quant Spectrosc Radiat Transf 2014;136:119–136. http://dx.doi.org/10.1016/j.jqsrt.2013.11.019.

[19] Birk M, Wagner G. Temperature-dependent air broadening of water in the 1250–1750 cm^{-1} range. J Quant Spectrosc Radiat Transf 2012;113:889–928. http://dx.doi.org/10.1016/j.jqsrt.2011.12.013.

[20] Coudert LH, Wagner G, Birk M, Baranov YI, Lafferty WJ, Flaud JM. The $H_2{}^{16}O$ molecule: line position and line intensity analyses up to the second triad. J Mol Spectrosc 2008;251:339–357. http://dx.doi.org/10.1016/j.jms.2008.03.021.

[21] Gordon IE, et al. The HITRAN 2016 molecular spectroscopic database. J Quant Spectrosc Radiat Transf.

[22] Loos J, Birk M, Wagner G. Measurement of positions, intensities and self-broadened line shape parameters of H_2O lines in the spectral ranges 1850–2280 cm^{-1} and 2390–4000 cm^{-1}. J Quant Spectrosc Radiat Transf 2017. http://dx.doi.org/10.1016/j.jqsrt.2017.02.013 (In press, This volume).

[23] Loos J. Verbesserung der spektroskopischen Datenbasis von H_2O für die Anwendungin bodengengebundener Fernerkundung der Atmosphëre [Ph.D. thesis]. Karlsuhe Institute for Technologie (KIT); 2017.

[24] Birk M, Loos J, Wagner G, Mondelain D, Kassi S, Campargue A, et al. Spectroscopic database for TROPOMI/Sentinel-5 precursor-2.3 μm region finalized. In: Proceedings of the ESA living planet symposium. Prague, Czech Republic; 2016. URL ⟨http://lps16.esa.int/⟩.

[25] Birk M, Wagner G, Loos J. Spectroscopy at 2.3 μm: analysis of ambient and low temperature pure CH4 measurements. In: Proceedings of the 13th ASA conference (united with 14th HITRAN conference). 13th ASA conference (united with 14th HITRAN conference). Reims, France; 2016. URL ⟨http://www.univ-reims.fr/minisite_35/home-accueil/asa-hitran-2016,18642,32042,html⟩.

[26] Wagner G, Birk M, Schreier F, Flaud J-M. Spectroscopic database for ozone in the fundamental spectral regions. J Geophys Res 2002;D22:4626. http://dx.doi.org/10.1029/2001JD000818.

[27] Toth RA. ν_2 band of $H_2{}^{16}O$ – line strengths and transition frequencies. J Opt Soc Am B 1991;8:2236–2255.

[28] Toth RA. $2\nu_2$-ν_2 and $2\nu_2$ bands of $H_2{}^{16}O$, $H_2{}^{17}O$, and $H_2{}^{18}O$: line positions and strengths. J Opt Soc Am B 1993;10:1526–1544.

[29] Toth RA. ν_1-ν_2, ν_3-ν_2, ν_1 and ν_3 bands of $H_2{}^{16}O$: line positions and strengths. J Opt Soc Am B 1993;10:2006–2029.

[30] Coudert LH, Martin-Drumel M-A, Pirali O. Analysis of the high-resolution water spectrum up to the second triad and to J=30. J Mol Spectrosc 2014;303:36–41. http://dx.doi.org/10.1016/j.jms.2014.07.003.

[31] Jacquinet-Husson N, Armante R, Scott NA, Chédin A, Crépeau L, Boutammine C, et al. The 2015 edition of the GEISA spectroscopic database. J Mol Spectrosc 2016;327:31–72. http://dx.doi.org/10.1016/j.jms.2016.06.007.

[32] Boone CD, Walker KA, Bernath PF. Speed-dependent Voigt profile for water vapor in infrared remote sensing applications. J Quant Spectrosc Radiat Transf 2007;105:525–532.

[33] Brown LR, Toth RA, Dulick M. Empirical line parameters of $H_2{}^{16}O$ near 0.94 μm: positions, intensities, and air-broadening coefficients. J Mol Spectrosc 2002;212:57–82.

[34] Grechko M, Boyarkin OV, Rizzo TR, Maksyutenko P, Zobov NF, Shirin S, et al. State-selective spectroscopy of water up to its first dissociation limit. J Chem Phys 2009;131:221105.

[35] Lisak D, Hodges JT, Low-uncertainty H. Low-uncertainty H_2O line intensities for the 930-nm region. J Mol Spectrosc 2008;249:6–13.

[36] Ngo NH, Lisak D, Tran H, Hartmann J-M. An isolated line-shape model to go beyond the Voigt profile in spectroscopic databases and radiative transfer codes. J Quant Spectrosc Radiat Transf 2013;129:89–100. http://dx.doi.org/10.1016/j.jqsrt.2013.05.034.

[37] Ngo NH, Lisak D, Tran H, Hartmann J-M. Erratum to An isolated line-shape model to go beyond the Voigt profile in spectroscopic databases and radiative transfer codes [J. Quant. Spectrosc. Radiat. Transf. 129 (2013) 89–100]. J Quant Spectrosc Radiat Transf 2014;134:105. http://dx.doi.org/10.1016/j.jqsrt.2013.10.016.

[38] Tran H, Ngo NH, Hartmann J-M. Efficient computation of some speed-dependent isolated line profiles. J Quant Spectrosc Radiat Transf 2013;129:199–203.

[39] Tran H, Ngo NH, Hartmann J-M. Erratum to Efficient computation of some speed-dependent isolated line profiles [J. Quant. Spectrosc. Radiat. Transfer 129 (2013) 199–203]. J Quant Spectrosc Radiat Transf 2014;134:104. http://dx.doi.org/10.1016/j.jqsrt.2013.10.015.

[40] Tennyson J, Bernath PF, Campargue A, Császár AG, Daumont L, Gamache RR, et al. Recommended isolated-line profile for representing high-resolution spectroscopic transitions (IUPAC Technical Report). Pure Appl Chem. 86; 2014. p. 1931–43. http://dx.doi.org/10.1515/pac-2014-0208.

[41] Hase F, Blumenstock T, Paton-Walsh C. Analysis of the instrumental line shape of high-resolution Fourier transform IR spectrometers with gas cell measurements and new retrieval software. Appl Opt 1999;38:3417. http://dx.doi.org/10.1364/AO.38.003417.

[42] Toth RA. Measurements of positions, strengths and self-broadened widths of H_2O from 2900 to 8000 cm^{-1}: line strength analysis of the 2nd triad bands. J Quant Spectrosc Radiat Transf 2005;94:51–107.

[43] Mikhailenko SN, Tyuterev VG, Keppler KA, Winnewisser BP, Winnewisser M, Mellau G, et al. The $2\nu_2$ band of water: analysis of new FTS measurements and high-K_a transitions and energy levels. J Mol Spectrosc 1997;184:330–349.

[44] Mikhailenko SN, Tyuterev VG, Starikov VI, Albert KK, Winnewisser BP, Winnewisser M, et al. Water spectra in the region 4200–6250 cm^{-1}; extended analysis of ν_1, ν_2, ν_2, ν_3, and $3\nu_2$ bands and confirmation of highly excited states from flame spectra and from atmospheric long-path observations. J Mol Spectrosc 2002;213:91–121.

[45] Jenouvrier A, Daumont L, Régalia-Jarlot L, Tyuterev VG, Carleer M, Vandaele AC, et al. Fourier transform measurements of water vapor line parameters in the 4200–6600 cm^{-1} region. J Quant Spectrosc Radiat Transf 2007;105:326–355.

[46] Vidler M, Tennyson J. Accurate partition function and thermodynamic data for water. J Chem Phys 2000;113:9766–9771.

[47] Furtenbacher T, Szidarovszky T, Hruby J, Kyuberis AA, Zobov NF, Polyansky OL, et al. Definitive high-temperature ideal-gas thermochemical functions of the $H_2{}^{16}O$ molecule. J Phys Chem Ref Data 2016;45:043104. http://dx.doi.org/10.1063/1.4967723.

[48] Chung H-K, Braams BJ, Bartschat K, Császár AG, Drake GWF, Kirchner T, et al. Uncertainty estimates for theoretical atomic and molecular data. J Phys D: Appl Phys 2016;49(36):363002. http://dx.doi.org/10.1088/0022-3727/49/36/363002.

[49] Zak E, Tennyson J, Polyansky OL, Lodi L, Tashkun SA, Perevalov VI. A room temperature CO_2 line list with ab initio computed intensities. J Quant Spectrosc Radiat Transf 2016;177:31–42. http://dx.doi.org/10.1016/j.jqsrt.2015.12.022.

[50] Zak EJ, Tennyson J, Polyansky OL, Lodi L, Zobov NF, Tashkun SA, et al. Room temperature line lists for CO_2 symmetric isotopologues with ab initio computed intensities. J Quant Spectrosc Radiat Transf 2017;189:267–280. http://dx.doi.org/10.1016/j.jqsrt.2016.11.022.

[51] Zak EJ, Tennyson J, Polyansky OL, Lodi L, Zobov NF, Tashkun SA, et al. Room temperature line lists for CO_2 asymmetric isotopologues with ab initio computed intensities, J Quant Spectrosc Radiat Transf. http://dx.doi.org/10.1016/j.

Please cite this article as: Birk M, et al. Accurate line intensities for water transitions in the infrared: Comparison of theory and experiment. J Quant Spectrosc Radiat Transfer (2017), http://dx.doi.org/10.1016/j.jqsrt.2017.03.040

jqsrt.2017.01.037.
[52] Assafrao D, Mohallem JR. The isotopic dipole moment of HDO. J Phys B: Mol Opt Phys 2007;40:F85–F91. http://dx.doi.org/10.1088/0953-4075/40/5/F02.
[53] Bubukina II, Polyansky OL, Zobov NF, Yurchenko SN. Optimized semiempirical potential energy surface for $H_2{}^{16}O$ up to 26,000 cm^{-1}. Opt Spectrosc 2011;110:160–166. http://dx.doi.org/10.1134/S0030400X11020032.
[54] Barletta P, Shirin SV, Zobov NF, Polyansky OL, Tennyson J, Valeev EF, et al. CVRQD adiabatic ab initio ground-state potential surfaces for the water molecule. J Chem Phys 2006;125:204307.
[55] Tennyson J. Vibration-rotation transition intensities from first principles. J Mol Spectrosc 2014;298:1–6. http://dx.doi.org/10.1016/j.jms.2014.01.012.
[56] Grechko M, Aseev O, Rizzo TR, Zobov NF, Lodi L, Tennyson J, et al. Stark coefficients for highly excited rovibrational states of H_2O. J Chem Phys 2012;136:244308.
[57] Tennyson J, Kostin MA, Barletta P, Harris GJ, Polyansky OL, Ramanlal J, et al. DVR3D: a program suite for the calculation of rotation-vibration spectra of triatomic molecules. Comput Phys Commun 2004;163:85–116.
[58] Zobov NF, Belmiloud D, Polyansky OL, Tennyson J, Shirin SV, Carleer M, et al. The near ultraviolet rotation-vibration spectrum of water. J Chem Phys 2000;113:1546–1552.
[59] Tolchenov RN, Naumenko O, Zobov NF, Shirin SV, Polyansky OL, Tennyson J, et al. Water vapor line assignments in the 9250–26,000 cm^{-1} frequency range. J Mol Spectrosc 2005;233:68–76.
[60] Dupre P, Germain T, Zobov NF, Tolchenov RN, Tennyson J. Continuous Wave-Cavity ring down near ultraviolet rotation-vibration spectrum of water. J Chem Phys 2005;123:154307. http://dx.doi.org/10.1063/1.2055247.
[61] Medvedev ES, Meshkov VV, Stolyarov AV, Gordon IE. Peculiarities of high-overtone transition probabilities in carbon monoxide. J Chem Phys 2015;143:154301. http://dx.doi.org/10.1063/1.4933136.
[62] Lampel J, Pöhler D, Polyansky OL, Kyuberis AA, Zobov NF, Tennyson J, et al. Detection of water vapour absorption around 363 nm in measured atmospheric absorption spectra and its effect on DOAS evaluations. Atmos Chem Phys 2017;17:1271–1295. http://dx.doi.org/10.5194/acp-2016-388.
[63] Rothman LS, Gordon IE, Barbe A, Benner DC, Bernath PF, Birk M, et al. The HITRAN 2008 molecular spectroscopic database. J Quant Spectrosc Radiat Transf 2009;110:533–572.
[64] J. Birks, Tech. rep.; 2001. [Accessed 16 March 2077]. [link]. URL ⟨http://www-naweb.iaea.org/napc/ih/documents/userupdate/Waterloo/⟩.
[65] Kyuberis AA, Zobov NF, Naumenko OV, Voronin BA, Polyansky OL, Lodi L, et al. Room temperature linelists for deuterated water. J Quant Spectrosc Radiat Transf., this issue.
[66] Barkan E, Luz B. High precision measurements of $^{17}O/^{16}O$ and $^{18}O/^{16}O$ ratio in H_2O. Rapid Commun Mass Spectrom 2005;19:3737–3742. http://dx.doi.org/10.1002/rcm.2250.
[67] Lodi L, Tennyson J. A line list of allowed and forbidden rotational transitions for water. J Quant Spectrosc Radiat Transf 2008;109:1219–1233.
[68] Rothman LS, Jacquemart D, Barbe A, Benner DC, Birk M, Brown LR, et al. The HITRAN 2004 molecular spectroscopic database. J Quant Spectrosc Radiat Transf 2005;96:139–204.
[69] Lynas-Gray AE, Miller S, Tennyson J. Infra red transition intensities for water: a comparison of ab initio and fitted dipole moment surfaces. J Mol Spectrosc 1995;169:458–467.
[70] Yurchenko SN, Tennyson J, Bailey J, Hollis MDJ, Tinetti G. Spectrum of hot methane in astronomical objects using a comprehensive computed line listz. Proc Nat Acad Sci USA 2014;111:9379–9383. http://dx.doi.org/10.1073/pnas.1324219111.

Please cite this article as: Birk M, et al. Accurate line intensities for water transitions in the infrared: Comparison of theory and experiment. J Quant Spectrosc Radiat Transfer (2017), http://dx.doi.org/10.1016/j.jqsrt.2017.03.040